Explicit expressions for the evolution of single-mode Rayleigh-Taylor and Richtmyer-Meshkov instabilities at arbitrary Atwood numbers

Karnig O. Mikaelian
University of California, Lawrence Livermore National Laboratory, Livermore, California 94551
(Received 22 August 2002; published 27 February 2003)

We present explicit analytic expressions for the evolution of the bubble amplitude in Rayleigh-Taylor (RT) and Richtmyer-Meshkov RM instabilities. These expressions are valid from the linear to the nonlinear regime and for arbitrary Atwood number A. Our method is to convert from the linear to the nonlinear solution at a specific value η^* of the amplitude for which explicit analytic expressions have been given previously for $A=1$ [K. O. Mikaelian, Phys. Rev. Lett. **80**, 508 (1998)]. By analyzing a recent extension of Layzer's theory to arbitrary A [V. N. Goncharov, Phys. Rev. Lett. **88**, 134502 (2002)], we find a simple transformation that generalizes our solutions to arbitrary A. We compare this model with another explicit model attributed to Fermi and with numerical simulations. Fermi's model agrees with numerical simulations for the RT case but its extension to the RM case disagrees with simulations. The model proposed here agrees with hydrocode calculations for both RT and RM instabilities.

DOI: 10.1103/PhysRevE.67.026319 PACS number(s): 47.20.−k

I. INTRODUCTION, NOTATION, AND SUMMARY

The purpose of this paper is to present simple, explicit, and analytic expressions for the evolution of perturbations in Rayleigh-Taylor (RT) [1] and Richtmyer-Meshkov (RM) [2] instabilities from the linear to the nonlinear regime. These instabilities have been extensively studied by analytical, numerical, as well as experimental techniques [3]. They have important applications in astrophysics [4], inertial-confinement fusion [5], and industry [6]. Despite this body of work we know of only one other analytic model that covers the linear as well as the nonlinear evolution explicitly, and it is the model that Layzer [7] attributed to Fermi.

RT and RM instabilities arise at the interface between two fluids subjected to a constant acceleration and a shock, respectively. The linear regime, during which the perturbation amplitude η remains much smaller than the perturbation wavelength λ, is well at hand as given by the original investigators [1,2]. Much of the subsequent research has focused on the nonlinear regime (but not all: issues of density gradients, ablation, compressibility, convergence, viscosity, material strength, etc., have been and continue to be actively researched in the linear regime; in this paper we ignore all such effects). Consequently, a great deal has been learned about the nonlinear regime. However, with the exception of Fermi's model noted above, we know of no explicit analytic model that describes the complete evolution.

There are, of course, several methods or models in which the solution to our problem is found by solving numerically an ordinary or partial differential equation(s), or by performing a sum over a large or infinite number of terms [8]. Our emphasis is on explicit analytical expressions for $\eta(t)$.

Following the notation of our earlier paper [9] we will consider four cases: two-dimensional (2D) and three-dimensional (3D) RT and RM. 2D flow is characterized by a wavelength λ and 3D flow by a tube radius R. The RT instability is characterized by a constant acceleration g, and the RM instability by a jump velocity Δv. We denote $\eta(0)$ by η_0, define wave number $k=2\pi/\lambda$, and Atwood number $A=(\rho_2-\rho_1)/(\rho_2+\rho_1)$, where ρ_i is the density of fluid i with the acceleration or jump velocity directed from the light fluid 1 towards the heavier fluid 2. In the linear regime we have

$$\text{2D RT:}\quad \eta(t)=\eta_0\cosh(\gamma t),\quad \gamma=\sqrt{gkA}, \tag{1a}$$

$$\text{3D RT:}\quad \eta(t)=\eta_0\cosh(\gamma t),\quad \gamma=\sqrt{g\beta_1 A/R}, \tag{1b}$$

$$\text{2D RM:}\quad \eta(t)=\eta_0(1+\Delta v kAt), \tag{2a}$$

$$\text{3D RM:}\quad \eta(t)=\eta_0(1+\Delta v \beta_1 At/R), \tag{2b}$$

where $\beta_1\approx 3.832$, the first zero of the Bessel function of order one. Note that 2D and 3D reduce to the same expressions if we identify k with β_1/R. This is not the identification made by Layzer; furthermore, in the nonlinear regime it will no longer be true that 3D results can be obtained from 2D results simply by identifying k with β_1/R.

The interface in 2D geometry is given by $y_0(x_0)=\eta_0\cos(kx_0)$, where y and x refer to the vertical and horizontal spatial dimensions that are parallel and perpendicular, respectively, to the direction of the acceleration or the shock. In 3D geometry, also called tubular flow (see Fig. 1 in Ref. [7]), the interface has the shape $z_0(r_0)=\eta_0 J_0(\beta_1 r_0/R)$ where z is the direction of the flow, r is in the radial direction, and J_0 is the Bessel function of order zero. Equations (1) and (2) are valid only in the linear, i.e., small-amplitude regime defined by $\eta k\ll 1$ and $\eta\beta_1/R\ll 1$ for 2D and 3D geometries, respectively. In this linear regime all results can be generalized from the $A=1$ case to arbitrary A simply by replacing g (or ΔV) by gA (or ΔVA). Again, this simple rule will no longer be true in the nonlinear regime (see below). Equations (1a), (1b), (2a), and (2b) were derived in Refs. [1,2,7,9], respectively. In addition to linearity, the above equations, like all equations in this paper, assume incompressible fluids.

Additional assumptions are necessary to obtain solutions in the nonlinear regime. For this purpose Layzer's model [7]

has been most fruitful. It assumes potential flow with the potential given by the first term in its Fourier expansion, and this is also the basis of our work [9]. It yields a second-order ordinary nonlinear differential equation. The model has been used extensively and compared successfully with hydrocode simulations. These comparisons have always relied on the numerical solution of the above-mentioned differential equation. What is new in this paper is that we present *analytic* solutions [Eqs. (3) and (10) below].

An alternate and somewhat adhoc, yet highly reasonable approach is attributed to Fermi by Layzer [7]: Assume that one knows the asymptotic bubble velocity $\dot{\eta}_\infty$ (in Fermi's time this was still under some dispute), then one may join the linear to the nonlinear regime by making an abrupt change in the growth rate $\dot{\eta}$. In other words, use the exponentially growing $\dot{\eta}_{\text{linear}}$ until it is equal to the asymptotic bubble velocity at which point $\dot{\eta}$ is replaced by the constant $\dot{\eta}_\infty$. We will compare our model with Fermi's model.

The rest of this paper treats the extension of Eqs. (1) and (2) to the nonlinear regime where $\eta(t)$ denotes the bubble amplitude, i.e., the penetration depth of the light fluid into the heavier fluid. Dimensional considerations indicate that there are only two independent parameters: $\eta_0 k$ (or $\eta_0 \beta_1 / R$) and A. In other words, if we scale η by k and t by $\sqrt{gk}$ for 2D RT, then the function we are seeking can be written as $\eta k(\sqrt{gk}t; \eta_0 k, A)$. It is similar for RM, where we scale t by $\Delta v k$.

We provide a brief summary. In Fermi's model [7] η is given by the linear regime until $\dot{\eta} = \dot{\eta}_\infty$, where $\dot{\eta}_\infty$ is the asymptotic bubble velocity, after which η is given by solving $\dot{\eta} = \dot{\eta}_\infty$. In our model η is given by the linear regime until $\eta = 1/3k$ (or $R/2\beta_1$ in 3D), after which η is given by a generalizied Layzer-type solution. Clearly, the transition from the linear to the nonlinear regime is based on $\dot{\eta}$ in Fermi's model and on η in ours. The asymptotic bubble velocity in both models is the same. Both models provide explicit analytic expressions where η and $\dot{\eta}$ vary continuously, as they must, during and after the transition. Although Fermi suggested his model for the RT case because at that time the RM instability was not yet identified (Richtmyer's paper appeared some five years after Layzer's), one can extend his principle to the RM case also. We find that for the RT case both models agree well with each other and with numerical simulations. For the RM case, however, Fermi's model predicts larger amplitudes while numerical simulations support the smaller amplitudes of our model.

In Sec. II we consider the RT case. The RM case is considered in Sec. III. The models are compared with numerical simulations using the CALE hydrocode [10] in Sec. IV where we also present our conclusions.

II. RT

It is interesting that the primary motivation for Layzer to develop his potential flow model was to compare with and evaluate Fermi's model, much as we are doing now. Layzer found [7] that Fermi's model "is never in error by more than about 25 per cent." Fermi's model is, needless to say, heuristic yet highly plausible. Layzer's method, on which this paper is based, can be described as using a simple potential in the fully nonlinear hydrodynamic equations. Despite its simplicity he could find analytically only the first integral ($\dot{\eta}$) and had to resort to numerical integration to find the second integral (η) and compare it with Fermi's model (see Fig. 2 in Ref. [7]). In retrospect, one can trace the difficulty of obtaining a second integral to Layzer's assumption of $\eta_0 = 0$ which he presumably made on the basis of simplicity. When we extended Layzer's work to arbitrary η_0 we found [9] that a first integral could still be derived analytically for any η_0. But what is more important and forms the crux of the present work, we discovered that if η_0 had a special value given by $1/3k$ in 2D and $R/2\beta_1$ in 3D, then a second integration could be performed analytically to obtain $\eta(t)$ explicitly.

Layzer's work and our extension of it were limited to one fluid only, i.e., $A = 1$. Recently Goncharov made a further extension to arbitrary A [11]. By analyzing his Eq. (8) for 2D and Eq. (18) for 3D we found first and second integrals *analytically for the same special values of* η_0:

$$\text{2D RT:}\quad \eta(t) = \eta_0 + \frac{3+A}{3(1+A)k}\ln \times\{\cosh[(6gkA(1+A))^{1/2}t/(3+A)] + (\dot{\eta}_0/\dot{\eta}_\infty) \times \sinh[(6gkA(1+A))^{1/2}t/(3+A)]\}, \tag{3a}$$

$$\text{3D RT:}\quad \eta(t) = \eta_0 + \frac{2R}{\beta_1(1+A)}\ln \times\{\cosh[(g\beta_1 A(1+A)/2R)^{1/2}t] + (\dot{\eta}_0/\dot{\eta}_\infty) \times \sinh[(g\beta_1 A(1+A)/2R)^{1/2}t]\}. \tag{3b}$$

These equations yield the following asymptotic bubble velocities in agreement with Goncharov [11] and Oron *et al.* [12]:

$$\text{2D RT:}\quad \dot{\eta}_\infty = \sqrt{\frac{2gA}{3(1+A)k}}, \tag{4a}$$

$$\text{3D RT:}\quad \dot{\eta}_\infty = \sqrt{\frac{2gAR}{(1+A)\beta_1}}. \tag{4b}$$

For $A = 1$ all equations in this paper reduce to their corresponding ones in Ref. [9]. In fact, we obtained the above solutions by the following transformation. Start with Eq. (7a) of Ref. [9] for $A = 1$ and let

$$g \to Ag\alpha, \quad k \to \frac{8(1+A)}{(3+A)^2}k/\alpha, \quad \eta \to \frac{(3+A)}{4}\eta\alpha \tag{5a}$$

to obtain Eq. (3a) above. Here α is an arbitrary parameter and the fact that Eq. (3a) is independent of α reflects the scaling behavior of $\eta k(\sqrt{gk}t;\eta_0 k,A)$ discussed in Sec. I. For 3D the transformation

$$g \rightarrow A g \alpha,$$

$$R \rightarrow \frac{2R\alpha}{1+A}, \tag{5b}$$

$$\eta \rightarrow \eta \alpha$$

converts Eq. (7b) of Ref. [9] into Eq. (3b) above.

In the model proposed here we use Eq. (1a) until $t=t^*$ when $\eta=\eta^*=1/3k$, i.e.,

$$t^* = \frac{1}{\gamma}\ln\left\{\frac{1}{3\eta_0 k}+\sqrt{\left(\frac{1}{3\eta_0 k}\right)^2-1}\right\},$$

$$\eta^* = 1/3k = \eta_0 \cosh(\gamma t^*),$$

$$\dot{\eta}^* = \eta_0 \gamma \sinh(\gamma t^*), \tag{6}$$

where $\gamma=\sqrt{gkA}$ and $\eta_0=\eta(t=0)$ is the actual initial amplitude here assumed to be less than or equal to $1/3k$, so there is some growth in the linear regime as given by Eq. (1a). At $t=t^*$ we switch to Eq. (3a) in which we replace η_0 by η^*, t by $t-t^*$, and $\dot{\eta}_0$ by $\dot{\eta}^*$, thus assuring the continuity of η and $\dot{\eta}$. A similar procedure is followed for 3D perturbations.

We now turn to Fermi's model given by linear growth, Eq. (1a), until $\dot{\eta}=\dot{\eta}_\infty$. Therefore,

$$t_F^* = \frac{1}{\gamma}\ln\left\{\frac{\dot{\eta}_\infty}{\eta_0\gamma}+\sqrt{\left(\frac{\dot{\eta}_\infty}{\eta_0\gamma}\right)^2+1}\right\},$$

$$\eta_F^* = \eta_0 \cosh(\gamma t_F^*) = \eta_0\sqrt{\left(\frac{\dot{\eta}_\infty}{\eta_0\gamma}\right)^2+1},$$

$$\dot{\eta}_F^* = \dot{\eta}_\infty. \tag{7}$$

Of course the growth after t_F^* is given by

$$\eta(t) = \eta_F^* + \dot{\eta}_\infty (t-t_F^*). \tag{8}$$

Comparing Eqs. (6) and (7), it is clear that the transition occurs later and therefore at a larger amplitude in Fermi's model. A good estimate of how much later is given by

$$\gamma(t_F^*-t^*) \approx \frac{1}{2}\ln\left(\frac{6}{1+A}\right) \tag{9}$$

assuming $\eta_0 k \ll 1$. In other words, the transition in Fermi's model is delayed by about 1/2 to 1 *e*-folding time.

Despite (or because of) this difference, the two models predict very similar behavior in amplitude. The reason is that there are compensating differences: In Fermi's model the transition from the linear regime is later but the saturation, by which we mean $\dot{\eta}=\dot{\eta}_\infty$, is immediate, while in our model the transition is earlier but the saturation occurs later as given by Eq. (3a) [compare with Eq. (8)].

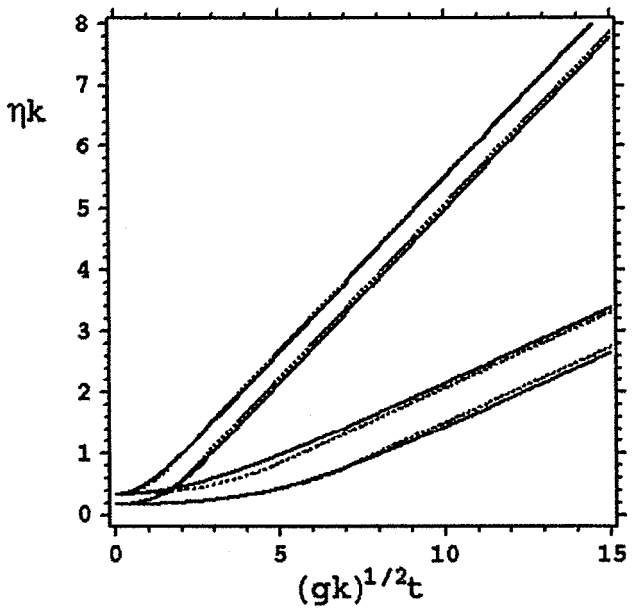

FIG. 1. Comparison of the present model (continuous curves) with Fermi's model (dotted curves) for the RT case. In the lower four curves $A=0.1$ with $\eta_0 k=\frac{1}{6}$ and $\frac{1}{3}$. In the upper four curves $A=0.9$ with $\eta_0 k=\frac{1}{6}$ and $\frac{1}{3}$.

In Fig. 1 we compare the two models for low and high Atwood numbers, $A=0.1$ and $A=0.9$, respectively. For each A we plot ηk as a function of $\sqrt{gk}t$ for two initial amplitudes: $\eta_0 k=1/6$ and 1/3. A comparison at intermediate A will be given in Sec. IV and compared with numerical simulations. It is clear from Fig. 1 that both models predict very similar $\eta(t)$.

III. RM

As pointed out by Richtmyer [2] the effect of a shock can be treated as the impulsive acceleration of incompressible fluids in which the effect of compressibility can be accounted for by using postshock amplitudes and Atwood numbers. We will adopt this approach, although there are rare cases where it fails [13]. Equation (2) gives the evolution in the linear regime. The nonlinear regime reduces to the RT problem with $g=0$. The resulting simplification allowed us to obtain first and second integrals for arbitrary η_0 (see Eqs. (10)–(15) in Ref. [9]). However, the solutions for $\eta_0 k=\frac{1}{3}$ or $\eta_0\beta_1/R=\frac{1}{2}$ were so simple that we propose using the same approach as in the previous RT section: Use the linear results until $\eta=1/3k$ or $R/2\beta_1$, at which time we switch to the following equations:

$$\text{2D RM:}\quad \eta(t) = \eta_0 + \frac{3+A}{3(1+A)k}\ln \times\{1+3\dot{\eta}_0 k t(1+A)/(3+A)\}, \tag{10a}$$

and

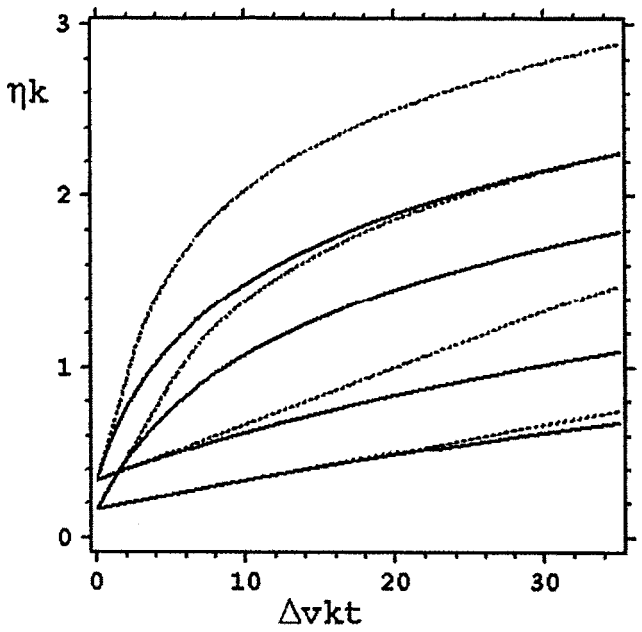

FIG. 2. Same as Fig. 1 for the RM case.

$$\text{3D RM:}\quad \eta(t)=\eta_0+\frac{2R}{(1+A)\beta_1}\ln\{1+\dot{\eta}_0\beta_1 t(1+A)/2R\}. \tag{10b}$$

These solutions are the $g=0$ versions of Eqs. (3a) and (3b), respectively. For the asymptotic bubble velocities they give

$$\text{2D RM:}\quad \dot{\eta}_\infty=\frac{3+A}{3(1+A)kt} \tag{11a}$$

and

$$\text{3D RM:}\quad \dot{\eta}_\infty=\frac{2R}{(1+A)\beta_1 t}. \tag{11b}$$

Our asymptotic velocities agree with the results of Oron *et al.* [12] and of Goncharov [11].

More explicitly, we use Eq. (2a) until $t=t^*$ when $\eta=\eta^*=1/3k$, i.e.,

$$t^*=\frac{1}{\Delta v kA}\left(\frac{1}{3\eta_0 k}-1\right),$$

$$\eta^*=1/3k,$$

$$\dot{\eta}^*=\eta_0\Delta v kA, \tag{12}$$

where $\eta_0=\eta(t=0+)$ is the postshock amplitude and A is the postshock Atwood number according to Richtmyer's prescription. At $t=t^*$ we switch to Eq. (10a) in which we replace η_0 by η^*, t by $t-t^*$, and $\dot{\eta}_0$ by $\dot{\eta}^*$, again assuring the continuity of η and $\dot{\eta}$. A similar procedure is followed for 3D perturbations.

Before we turn to a Fermi-inspired model, let us note here another model that illustrates the remarks made in Sec. I. Zhang and Sohn [14] proposed solving the fully compressible linear equations given by Richtmyer that give a more accurate description of the early evolution than the simple prescription given by Richtmyer himself. A similar model was proposed by Li and Zhang [15]. The difficulty, of course, is that these equations must be solved numerically as was done by Richtmyer and, more recently, by Yang, Zhang, and Sharp [16]. Second, by using second-order Padé approximants, the analytic part of the model in Ref. [14] is limited to the *weakly* nonlinear regime (for example, one obtains the wrong asymptotic velocity as pointed out earlier [9]). More accurate results are obtained by Velikovich and Dimonte [17] by going to much higher Padé approximants, but now the higher-order terms, even for a single incompressible fluid, must be computed numerically.

We turn to a Fermi-type approach. Indeed, the power of Fermi's model is that it can be applied to any instability whose $\dot{\eta}_\infty$ is known. Equating the right-hand side of Eq. (11a) to the linear growth rate $\eta_0\Delta v kA$ we have

$$t_F^*=\frac{3+A}{3(1+A)k^2\Delta vA\eta_0},$$

$$\eta_F^*=\eta_0\left(1+\frac{3+A}{3(1+A)k\eta_0}\right),$$

$$\dot{\eta}_F^*=\dot{\eta}_\infty(t^*)=\dot{\eta}_0=\eta_0\Delta v kA. \tag{13}$$

Note that since $\dot{\eta}_\infty$ is time dependent we cannot use Eq. (8) for $t>t^*$. In fact the evolution for $t>t^*$ is given by the *same* equation as in our model, Eq. (10a), in which η_0 is replaced by η_F^* and t by $t-t_F^*$. Since $\dot{\eta}$ is constant in the linear regime ($=\eta_0\Delta v kA$) we have $\dot{\eta}^*=\eta_F^*=\dot{\eta}_0$ in both models. Therefore, the only difference between our model and Fermi's model is the value of t^* (and hence η^*) where the transition occurs.

As in the RT case, it is easy to see that $t_F^*>t^*$ and $\eta_F^*>\eta^*$,

$$t_F^*/t^*=\frac{3+A}{(1+A)(1-3\eta_0 k)}, \tag{14}$$

and, assuming $\eta_0 k\ll 1$, the transition occurs 2 to 3 times later in Fermi's model than ours and therefore at about 2 to 3 times larger amplitude.

Since there is no compensating difference here, Fermi's model predicts substantially larger amplitudes than ours, as illustrated in Fig. 2. Numerical simulations presented in Sec. IV support the smaller amplitudes.

We close this section by noting that the formula

$$\dot{\eta}=\frac{\dot{\eta}_0}{1+\dot{\eta}_0/\dot{\eta}_\infty} \tag{15}$$

captures both 2D and 3D RM growth rates in the nonlinear regime [see Eqs. (10a)–(11b)].

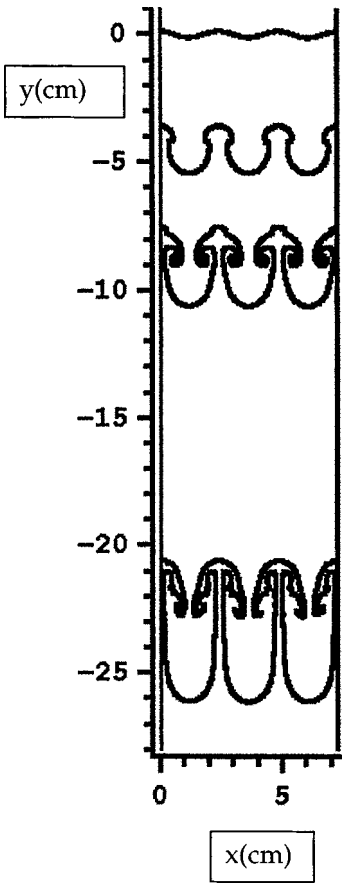

FIG. 3. Snapshots from a CALE simulation: $g=70\ g_0=0.0686$ cm/ms^2, $\lambda=2.43$ cm, $\eta_0=0.13$ cm. The width of the tank is 7.3 cm or $3\times\lambda$. The upper fluid is hexane ($\rho=0.66$ g/cm^3), the lower fluid is a water/NaI solution ($\rho=1.87$ g/cm^3). Snapshots at $t=0$, 15, 20, and 30 ms.

IV. NUMERICAL SIMULATIONS AND CONCLUSIONS

Layzer's model has been found to agree well with more accurate solutions requiring numerical integration. The earliest comparison was reported by Birkhoff and Carter [18] who found

$$\dot{\eta}_\infty=(0.23\pm0.01)\sqrt{g\lambda} \tag{16}$$

for 2D RT and $A=1$, compared with $\sqrt{g\lambda/6\pi}$ from Eq. (4a). Recent comparisons [19] continue to show good agreement (see also Refs. [9] and [11]).

We have carried out 2D direct numerical simulations of RT and RM instabilities on the CALE hydrocode [10]. For RT we chose the linear electric motor system of Dimonte and Schneider [20] (DS) with somewhat idealized conditions: The acceleration increases from 0 to $70g_0$ ($g_0=0.98\times10^{-3}$ cm/ms^2) in 7 ms, after which it is kept constant at that value. Three identical sinusoidal perturbations are initiated at the center of the numerical tank, which is 7.3 cm wide, hence $\lambda\approx2.43$ cm, with initial amplitudes $\eta_0=0.065$ cm or 0.13 cm ($\eta_0k\approx\frac{1}{6}$ or $\frac{1}{3}$). We chose $\rho_1=0.66$ g/cm^3 and $\rho_2=1.87$ g/cm^3 corresponding to fill No. 31 in DS (see the second paper in Ref. [20]), hence $A\approx0.48$. The calculations are stopped at 30 ms when the spikes approach the top of the 8.8-cm-long tank. Snapshots of the calculation for $\eta_0k=\frac{1}{3}$ are shown in Fig. 3.

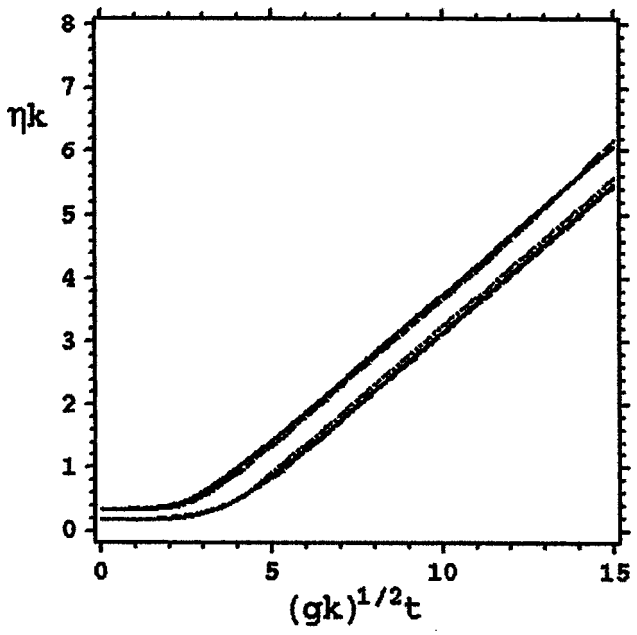

FIG. 4. Comparison of hydrocode and analytic results for the RT case with $A=0.48$. The solid curves are from the model presented in this paper, the dotted curves are from Fermi's model, and the dashed curves are from the CALE simulations. The lower three curves are for $\eta_0=0.065$ cm; the upper three curves are for $\eta_0=0.13$ cm. Snapshots from the hydrocode simulations are shown in Fig. 3.

To compare the simulation with analytical models, we use

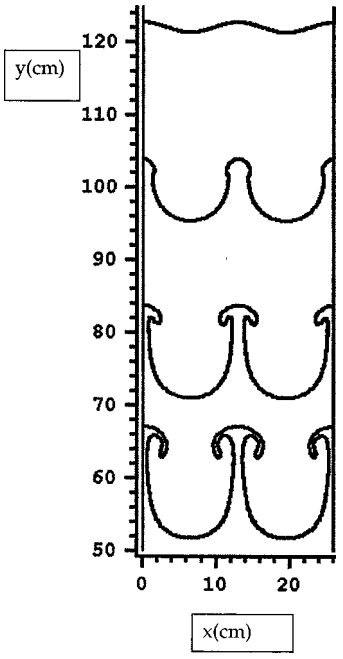

FIG. 5. Snapshots from a CALE simulation of a shock tube: a Mach 1.2 shock in helium strikes the He/air interface with perturbations of $\lambda=13$ cm, $\eta_0=0.7$ cm, located 122 cm away from the endwall placed at $y=0$. Snapshots at $t=0$, 1.5, 3.0, and 4.2 ms.

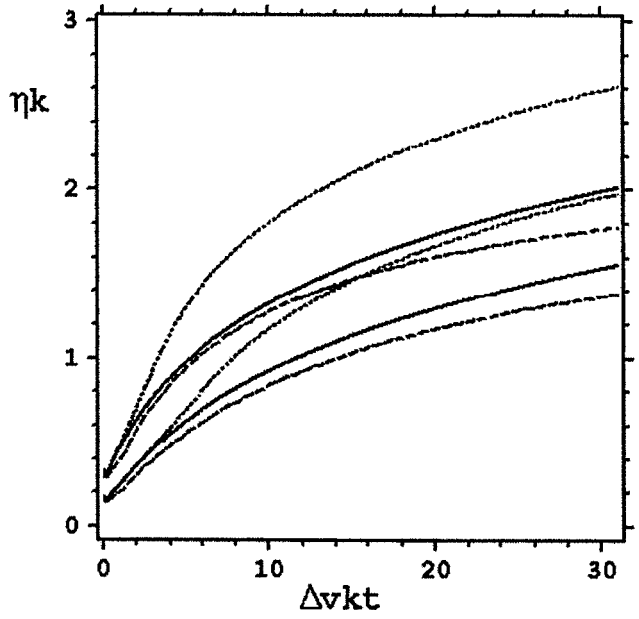

FIG. 6. Comparison of hydrocode and analytic results for the RM case with $A=0.77$. The solid curves are from the model presented in this paper, the dotted curves are from Fermi's model, and the dashed curves are from the CALE simulations. The lower three curves are for $\eta_0=0.35$ cm; the upper three curves are for $\eta_0=0.7$ cm. Snapshots from the hydrocode simulations are shown in Fig. 5.

a constant $g(=70g_0)$ and, since the tank takes 7 ms to reach this constant value we shift the origin of time by 3.5 ms. In Fig. 4 we display the bubble amplitude from the simulations, Fermi's model, and the present model. Clearly, the simulations and the models agree well with each other for the smaller as well as the larger amplitude.

For RM simulations we use the same extended version of the Cal Tech shock tube [21] as in our earlier work: a Mach 1.2 shock propagating in He strikes a He/air interface with perturbations of $\lambda=13$ cm (two identical perturbations in a 26-cm-wide shock tube) and $\eta_0=0.35$ cm or 0.70 cm ($\eta_0 k \approx \frac{1}{6}$ or $\frac{1}{3}$). The results for the high Atwood number He/Xe system were reported in Ref. [9]. For the present He/air system $A_{\text{before}}=0.76$ and $A_{\text{after}}\approx 0.77$. The jump velocity is $\Delta v \approx 15.8$ cm/ms and, since the incident shock speed in He is $W_i \approx 121$ cm/ms, the compression factor is $1-\Delta v/W_i \approx 0.87$. The interface is initially 122 cm away from the endwall and, by 4.2 ms, is about 55 cm away from it. The calculations are stopped at this time because a shock, reflected from the endwall, is only 5 cm away from the interface and reshocks the interface shortly after 4.2 ms.

Snapshots from the CALE simulations are given in Fig. 5. In Fig. 6 we compare the bubble amplitudes from the simulations and the two models discussed in the preceding section. Fermi's model clearly overestimates the growth while our model based on $\eta^*=1/3k$ shows good agreement with the simulations to within $\sim$10% for both the smaller and larger amplitude runs.

To conclude, we have capitalized on the explicit analytic solutions found for special values of η_0 to transition continuously from the linear to the nonlinear and far asymptotic regimes. A similar transition can be done in Fermi's model where the criterion for transition is based on $\dot{\eta}$ rather than η. The two models agree with each other and with simulations for the RT case, but for the RM case our model gives better agreement with numerical simulations. We suggest using Eqs. (3) and (10) whenever explicit analytic expressions are needed for RT and RM instabilities.

ACKNOWLEDGMENTS

I am grateful to V. Goncharov, C. Cherfils, and J. Ramshaw for discussions, and to O. Schilling for references. This work was performed under the auspices of the U.S. Department of Energy at the University of California Lawrence Livermore National Laboratory under Contract No. W-7405-Eng-48.

[1] Lord Rayleigh, *Scientific Papers* (Dover, New York, 1965), Vol. 2; G. I. Taylor, Proc. R. Soc. London, Ser. A **201**, 192 (1950).

[2] R. D. Richtmyer, Commun. Pure Appl. Math. **13**, 297 (1960); E. E. Meshkov, Izv. Akad. Nauk SSR, Mekh. Zhidk. Gaza **5**, 151 (1969) [Fluid Dyn. **4**, 101 (1969)].

[3] There is vast literature on RT and RM instabilities. We mention a few reviews: D. H. Sharp, Physica D **12**, 3 (1984); H. J. Kull, Phys. Rep. **206**, 197 (1991); M. Brouillette, Annu. Rev. Fluid Mech. **34**, 445 (2002). Active research in these fields is reported in *Proceedings of the Seventh International Workshop on The Physics of Compressible Turbulent Mixing, St. Petersburg, Russia*, 1999, edited by E. Meshkov, Yu. Yanilkin, and V. Zhmailo (RFNC-VNIIEF, Sarov, Russia, 2001).

[4] B. A. Remington, R. P. Drake, H. Takabe, and D. Arnett, Phys. Plasmas **7**, 1641 (2000).

[5] J. D. Lindl, *Inertial Confinement Fusion* (Springer-Verlag, New York, 1998).

[6] B. J. Kim and M. Corradini, Nucl. Sci. Eng. **98**, 16 (1988).

[7] D. Layzer, Astrophys. J. **122**, 1 (1955). Reference to Fermi's model is found here.

[8] B. J. Daly, Phys. Fluids **10**, 297 (1967); G. R. Baker, D. I. Meiron, and S. A. Orszag, *ibid.* **23**, 1485 (1980); J. W. Jacobs and I. Catton, J. Fluid Mech. **187**, 329 (1988); H. Aref and G. Tryggvason, Phys. Rev. Lett. **62**, 749 (1989); G. Hazak, *ibid.* **76**, 4167 (1996); M. Vandenboomgaerde, S. Gauthier, and C. Mügler, Phys. Fluids **14**, 1111 (2002). See also Refs. [12,14,15,17–19].

[9] K. O. Mikaelian, Phys. Rev. Lett. **80**, 508 (1998).

[10] R. E. Tipton, CALE Users Manual (unpublished).

[11] V. N. Goncharov, Phys. Rev. Lett. **88**, 134502 (2002).

[12] D. Oron, L. Arazi, D. Kartoon, A. Rikanati, U. Alon, and D. Shvarts, Phys. Plasmas **8**, 2883 (2001).

[13] K. O. Mikaelian, Phys. Rev. Lett. **71**, 2903 (1993); Phys. Fluids **6**, 536 (1994).

[14] Q. Zhang and S.-I. Sohn, Phys. Lett. A **212**, 149 (1996).

[15] X. L. Li and Q. Zhang, Phys. Fluids **9**, 3069 (1997).
[16] Y. Yang, Q. Zhang, and D. H. Sharp, Phys. Fluids **6**, 1856 (1994).
[17] A. L. Velikovich and G. Dimonte, Phys. Rev. Lett. **76**, 3112 (1996).
[18] G. Birkhoff and D. Carter, J. Math. Mech. **6**, 769 (1957).
[19] J. Hecht, U. Alon, and D. Shvarts, Phys. Fluids **6**, 4019 (1994).
[20] G. Dimonte and M. Schneider, Phys. Rev. E **54**, 3740 (1996); Phys. Fluids **12**, 304 (2000).
[21] M. Vetter and B. Sturtevant, Shock Waves **4**, 247 (1995).